Acta Oceanol. Sin., 2017, Vol. 36, No. 7, P. 48–55
DOI: 10.1007/s13131-016-1083-2
http://www.hyxb.org.cn
E-mail: hyxbe@263.net

Characterization of iron diagenesis in marine sediments using refined iron speciation and quantized iron(III)-oxide reactivity: a case study in the Jiaozhou Bay, China

TAO Jing[1], MA Weiwei[1], ZHU Maoxu[1]*, LI Tie[1], YANG Rujun[1]

[1] College of Chemistry and Chemical Engineering, Ocean University of China, Qingdao 266100, China

Received 21 April 2016; accepted 2 December 2016

©The Chinese Society of Oceanography and Springer-Verlag Berlin Heidelberg 2017

Abstract

As a case study, refined iron (Fe) speciation and quantitative characterization of the reductive reactivity of Fe (III) oxides are combined to investigate Fe diagenetic processes in a core sediment from the eutrophic Jiaozhou Bay. The results show that a combination of the two methods can trace Fe transformation in more detail and offer nuanced information on Fe diagenesis from multiple perspectives. This methodology may be used to enhance our understanding of the complex biogeochemical cycling of Fe and sulfur in other studies. Microbial iron reduction (MIR) plays an important role in Fe(III) reduction over the upper sediments, while a chemical reduction by reaction with dissolved sulfide is the main process at a deeper (> 12 cm) layer. The most bioavailable amorphous Fe(III) oxides [$Fe(III)_{am}$] are the main source of the MIR, followed by poorly crystalline Fe(III) oxides [$Fe(III)_{pc}$)] and magnetite. Well crystalline Fe(III) oxides [$Fe(III)_{wc}$] have barely participated in Fe diagenesis. The importance of the MIR over the upper layer may be a combined result of the high availability of highly reactive Fe oxides and low availability of labile organic matter, and the latter is also the ultimate factor limiting sulfate reduction and sulfide accumulation in the sediments. Microbially reducible Fe(III) [MR-Fe(III)], which is quantified by kinetics of Fe(II)-oxide reduction, mainly consists of the most reactive $Fe(III)_{am}$ and less reactive $Fe(III)_{pc}$. The bulk reactivity of the MR-Fe(III) pool is equivalent to aged ferrihydrite, and shows down-core decrease due to preferential reduction of highly reactive phases of Fe oxides.

Key words: iron oxides, Jiaozhou Bay in China, marine sediments, microbial iron reduction, reactivity, speciation

Citation: Tao Jing, Ma Weiwei, Zhu Maoxu, Li Tie, Yang Rujun. 2017. Characterization of iron diagenesis in marine sediments using refined iron speciation and quantized iron(III)-oxide reactivity: a case study in the Jiaozhou Bay, China. Acta Oceanologica Sinica, 36(7): 48–55, doi: 10.1007/s13131-016-1083-2

1 Introduction

Iron (Fe) is one of the four elements (along with sulfur, oxygen, and organic carbon) dominating diagenetic reactions and redox conditions in coastal sediments. As a result, Fe redox cycling exerts profound influences on fate of carbon, sulfur (S), phosphorus, and a multitude of trace elements (Raiswell and Canfield, 2012). In anoxic marine settings, Fe(III) oxides are reduced by two competitive pathways: microbial iron(III) reduction (MIR) coupled to organic matter (OM) oxidation and chemical iron(III) reduction (CIR) by mainly dissolved sulfide produced by sulfate reduction (i.e., abiotic reduction) (Canfield et al., 2005; Lovley, 1991). The CIR generally dominates over the MIR in OM-rich marine settings due to quick reduction of Fe(III) oxides by dissolved sulfide (Jacobson, 1994; Koretsky et al., 2003), and consequently the MIR is prevalent only in marine sediments where porewater sulfide is limited in the conditions of a low sulfate reduction rate and/or quick sulfide consumption by reaction with reactive Fe(III) oxides (Wang and van Cappellen, 1996; Wijsman et al., 2002). However, mounting evidence indicates that the MIR plays a much more important role than previously recognized in sediments of many marine settings (Beckler et al., 2016; Devereux et al., 2015; Jensen et al., 2003; Kristensen et al., 2011; Rysgaard et al., 2001).

The relative importance of the CIR vs the MIR in a given sediments depends on a number of interwoven factors, particularly the reactivity of Fe(III) oxides and the availability of labile OM. Amorphous and poorly crystalline Fe(III) oxides are usually regarded as highly reactive Fe (FeO_{HR}) pool, and they are always preferentially involved in both CIR and MIR. Thus the reactivity and availability of Fe oxides are critical in controlling the intensity and pathways of Fe redox cycling. The availability of labile OM is also critical in regulating Fe redox cycling. The high availability of labile OM generally stimulates sulfate reduction. In this case, sufficient supply of dissolved sulfide favors the CIR but impresses the MIR. It follows that the CIR predominates over the MIR in sediments underlying eutrophicated waters because of enhanced supply of OM to the sea floor. This feature has been confirmed in several studies (Zimmerman and Canuel, 2000; Kraal et al., 2013), furthermore, the MIR has still been observed to play some role in Fe reduction in some eutrophicated marine settings (Hyun et al., 2013). Further work is needed to tease out the key factors regulating the pathways of the CIR vs the MIR and their relative importance.

Up to date, no direct geochemical methods are available to

Foundation item: The National Natural Science Foundation of China under contract Nos 41576078 and 41276069; the Shandong Province Natural Science Foundation of China under contract No. ZR2015DM006; the National Key Research and Development Program of China under contract No. 2016YFA0601301.
*Corresponding author, E-mail: zhumaoxu@ouc.edu.cn

quantify the MIR in marine sediments because the CIR and the MIR cannot be clearly identified from the product of Fe(III) reduction, i.e., Fe(II). Microbiological methods including pure/slurry incubation and enumeration techniques have often been used to infer relative changes of population sizes and activity of Fe reducing bacteria *in situ*. But those techniques provide only a partial view because some groups of microorganisms resist cultivation (Amann et al., 1997), and a microbial community size does not necessarily correlate with its activity (Koretsky et al., 2005; Luna et al., 2002). Studies have demonstrated that the quantification of reactivity and availability of microbially reducible Fe(III) (MR-Fe(III)) based on the kinetics of reductive dissolution can provide useful information on the MIR (Chen et al., 2013; Hyacinthe et al., 2006; Hyacinthe and van Cappellen, 2004; Zhu et al., 2014b). Most recently, a Fe speciation method refined by Zhu et al. (2015) can also provide insights into processes of the CIR and the MIR. However, a combination of the two techniques has not been applied to investigating Fe diagenesis in sediments. In this study, one sediment core from the eutrophic Jiaozhou Bay was investigated as a case study by combining the two techniques to: (1) trace diagenetic processes of reactive Fe pools, (2) assess the importance of the CIR vs the MIR, and (3) quantitatively characterize MR-Fe(III). The study aims at setting an example for the application of the synthetic methodology for better understanding Fe cycling and also providing a more detailed context for further documenting Fe-related biogeochemical processes in marine sediments.

2 Study area and methods

2.1 *Study area and sampling*

The Jiaozhou Bay is a semienclosed water body linked by a narrow channel to the Yellow Sea (Fig. 1). High anthropogenic nutrient loadings from the rivers, notably the Dagu River, the Moshui River, and the Baisha River, have resulted in enhanced primary productivity and frequent occurrences of algal blooms in the bay since 1997 (Liu et al., 2005; Wu et al., 2005). Despite this, an increase in OM burial, as usually expected, has not been observed. Rather, a large-scale benthic shellfish mariculture in the bay has resulted in lower OM burial over the upper 30 cm relative to the deeper layer (Liu et al., 2010). It remains unclear whether the CIR is still the prevalent pathway in the bay as observed in many other coastal sediments impacted by eutophication, given the fact that OM burial has not been increased despite eutrophication of the water.

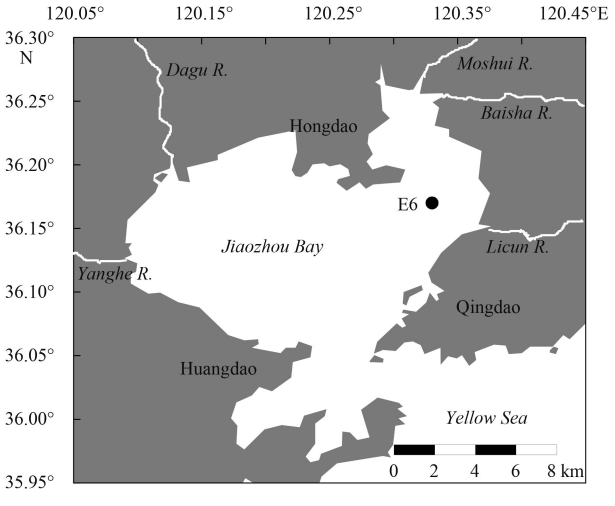

Fig. 1. Map of sampling Site E6 in the Jiaozhou Bay, China.

One sediment core (36.17°N, 120.33°E, water depth: 6 m) was collected using a box corer on May 21, 2012 (Fig. 1). After the retrieval of the box-core, two PVC tubes (inner diameter 8 cm, length 28 cm) were vertically inserted for tube coring, and then two ends of the cores were immediately covered and clasped with fitted tops. Upon transported to the laboratory within 4 h, the sediment cores were immediately sectioned at 1.5 cm interval over the upper 8 cm and at 4 cm interval below this depth in a N_2 glove box, and then sealed in zip-lock plastic bags and frozen at –18°C until further handling within two months. According to our previous studies in this study area (Zhu et al., 2012), the violent fluctuations of geochemical signatures generally occur within the upper 5–10 cm. So the core was sectioned at a small interval (1.5 cm) over the upper 8 cm to capture potential geochemical fluctuations, while a larger interval (4 cm) was small enough to capture the gradual variations of the geochemical signatures below a depth of 8 cm. After thawing at the room temperature under N_2 atmosphere, subsamples were immediately subjected to treatments as described below.

2.2 *Total organic carbon analysis*

Preweighed wet sediment samples in duplicate were dried at 105°C in oven until constant weight for the gravimetric analysis of water contents. The contents of Fe and S in all extractions below were expressed in micromole per gram dry weight of sediments (μmol/g). Dry sediment subsamples of known mass (≈1 g) were treated with 1 mol/dm^3 HCl overnight and washed twice with deionized water to remove carbonates. The samples were then redried at approximately 60°C for 12 h and ground to approximately 100 mesh for total organic carbon (TOC) analysis using a PE2400II CN element analyzer, with relative deviations of duplicates better than 7.0%.

2.3 *Sulfur speciation*

Three S forms, that is, acid volatile sulfide (AVS), elemental sulfur (S^0), and pyrite-S, were quantified by chemical extractions. Operational procedures for the extractions have been detailed elsewhere (Zhu et al., 2012, 2013), and thus were only briefly presented here.

A mixed solution of 20 mL HCl (6 mol/dm^3) and 1 mL ascorbic acid (0.1 mol/dm^3) was employed to preweighed frozen wet sediments (≈1 g) in triplicate to release AVS in a closed reactor prepurged with N_2. Ascorbic acid was used to inhibit oxidization of AVS by simultaneously extracted Fe^{3+}. Evolved H_2S gas was precipitated as ZnS using the cool diffusion method (Burton et al., 2008), and was determined by a methylene blue method (Cline, 1969).

Residual sediment pellets after AVS removal above were rinsed twice using deionized water and then immediately treated with 20 mL acetone to extract S^0 under magnetic stirring for 24 h. After centrifugation (4 800 r/min) for 10 min and filtration (0.22 μm) the filtrates were left in fume hood for acetone vaporization. The S^0 was then reduced to H_2S gas by a cold acidic chromium(II) solution (48 h) in a closed reactor prepurged with N_2 (Burton et al., 2008; Kallmeyer et al., 2004; Zhu et al., 2013), and determined by the same method for the above AVS.

Pyrite-S in water-washed residual sediments after S^0 extraction was reduced to H_2S (48 h, with occasional magnetic stirring) with the cold acidic chromium(II) solution (Burton et al., 2008; Kallmeyer et al., 2004) and determined by the same method for S^0.

2.4 *Iron speciation*

A combination of several extraction techniques was used to achieve a refined speciation of five operational Fe phases: (1) buffered acetate-extractable Fe(II), (2) amorphous Fe(III) oxides ($Fe(III)_{am}$), (3) poorly crystalline Fe(III) oxides ($Fe(III)_{pc}$), (4) well crystalline Fe(III) oxides ($Fe(III)_{wc}$), and (5) magnetite (Fe_{mag}). All procedures for the refined extractions have been detailed in a companion paper (Zhu et al., 2015), and thus were only briefly described here (Fig. 2).

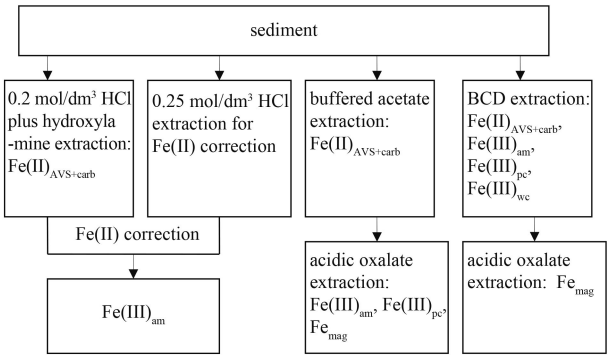

Fig. 2. Flow diagram for Fe extractions.

2.4.1 *Acidic hydroxylamine extraction*

Under N_2, mixing solution of HCl (0.25 mol/dm^3) and hydroxylamine (0.25 mol/dm^3) was added to preweighed (≈1 g) frozen wet sediments in triplicate for 1 h extraction while shaking. In the acidic condition, this brief extraction targeted mainly $Fe(III)_{am}$ through reductive dissolution, while H^+ presented in the solution also dissolved solid-phase Fe(II) (pyrite excluded) (Lovley and Phillips, 1987). Hence another subsample was extracted with 0.25 mol/dm^3 HCl solution by the same procedure described above to correct for H^+-promoted Fe dissolution in the acidic hydroxylamine extraction. Hydroxylamine extraction after correction represented an estimate of $Fe(III)_{am}$ (Lovley and Phillips, 1987).

2.4.2 *Buffered acetate extraction followed by acidic oxalate extraction*

Buffered acetate (pH 4.5) is capable of extracting AVS-bound Fe(II) [$Fe(II)_{AVS}$] and Fe(II) carbonates [$Fe(II)_{carb}$], for example, siderite and ankerite, but leaves most Fe (oxyhydr)oxides relatively unaffected (Poulton and Canfield, 2005). The acetate-extractable Fe(II) is thereafter denoted as acetate-Fe(II). Acidic oxalate is capable of extracting acetate-Fe(II), $Fe(III)_{am}$, $Fe(III)_{pc}$, and Fe_{mag} (Kostka and Luther III, 1994; Poulton and Canfield, 2005). Under N_2, preweighed frozen wet sediments in triplicate were subjected to buffered acetate (1 mol/dm^3) extraction to estimate the amount of acetate-Fe(II). Water-washed sediment residues after removal of the above acetate-Fe(II) were immediately subjected to a 6 h extraction by 0.2 mol/dm^3 oxalate (pH 3.2). In this case, oxalate-extractable Fe (oxalate-Fe) represented an estimate of the total amount of $\Sigma[Fe(III)_{am}+Fe(III)_{pc}+Fe_{mag}]$.

2.4.3 *Bicarbonate-citrate buffered sodium dithionite (BCD) extraction followed by acidic oxalate extraction*

BCD is capable of extracting acetate-Fe(II), $Fe(III)_{am}$, $Fe(III)_{pc}$, and $Fe(III)_{wc}$, but only minor Fe_{mag} (6%–7%) (Poulton and Canfield, 2005; Raiswell et al., 1994). Preweighed frozen wet sediments in triplicate were sequentially extracted by BCD (2 h) at 75°C and then by acidic oxalate (6 h). In this extraction, BCD-extractable Fe (BCD-Fe) represented the total amount of Σ[acetate-Fe(II)+$Fe(III)_{am}$+$Fe(III)_{pc}$+$Fe(III)_{wc}$], and the oxalate extraction represented Fe_{mag}.

All extracted Fe above was measured by colorimetry (Stookey, 1970). The above extraction protocol allows a further estimation of the amounts of $Fe(III)_{pc}$ and $Fe(III)_{wc}$:

$Fe(III)_{pc}$=oxalate-Fe–$\Sigma[Fe(III)_{am}+Fe_{mag}]$,

$Fe(III)_{wc}$=BCD-Fe–Σ[acetate-Fe(II)+$Fe(III)_{am}$+$Fe(III)_{pc}$].

2.5 *Kinetic dissolution of sedimentary iron oxides*

Natural Fe(III)-oxide assemblages with variable crystallinity and surface properties can be regarded as a continuum. Their reductive reactivity can be described by a gamma function, and the rate law of their reductive dissolution (Larsen and Postma, 2001; Postma, 1993) can be expressed as

$$\frac{J}{m_0} = k' \left(\frac{m}{m_0}\right)^{\gamma}, \tag{1}$$

where J is the reduction rate (μmol/s); k' is the apparent rate constant (s^{-1}) and hence is a measure of reductive reactivity; m_0 (μmol/g) is the theoretical initial mass of the reactive Fe(III) oxides studied; m is the remaining mass at a given time t; and γ is the apparent reaction order.

Integrated form of Eq. (1) for $\gamma \neq 1$ is

$$\frac{m}{m_0} = [-k'(1-\gamma)t + 1]^{\frac{1}{1-\gamma}}. \tag{2}$$

For the convenience of data processing, Eq. (2) is converted to as follows:

$$m_t = m_0\{1 - [1 - k'(1-\gamma)t]^{\frac{1}{1-\gamma}}\}, \tag{3}$$

where m_t is dissolved amounts at time t, that is, m_t=m_0–m.

In this study, the time-dependent dissolution of Fe(III) oxides in the Jiaozhou Bay sediments was conducted using bicarbonate-citrate (BC) buffered ascorbate (pH 7.5) as a reductant. Experimental procedures have been detailed previously (Chen et al., 2013; Zhu et al., 2014b). Briefly, a freshly thawed sediment of the known mass (7.5–8.5 g) was loaded into a reactor containing 950 mL buffered ascorbate solution (20 g/L). After immediate sealing, the suspension was kept purged with N_2 and magnetically stirred during 24-h experiments. The suspensions were sampled periodically using 2 mL syringes and filtrated (0.2 μm) to glass vials containing sodium-acetate-buffered ferrozine solution for later determination of Fe^{2+} by colorimetry (Stookey, 1970). The relative deviations of duplicates were less than 6%. The optimized values of m_0, k' and γ can be simultaneously determined by fitting kinetic data to Eq. (3), using nonlinear least squares procedure. According to Hyacinthe et al. (2006), the kinetic parameters derived from the chemical reduction (pH 7.5) bear specific microbial implications: k' can be used as a forecast proxy of microbial reactivity of Fe(III) oxides and m_0 as a maximum estimate of MR-Fe(III) present in the sediments.

3 Results

3.1 *TOC, sulfur and iron*

TOC content in the core was within a narrow range of 0.70%–0.81% with no clear depth variability (Fig. 3a). AVS con-

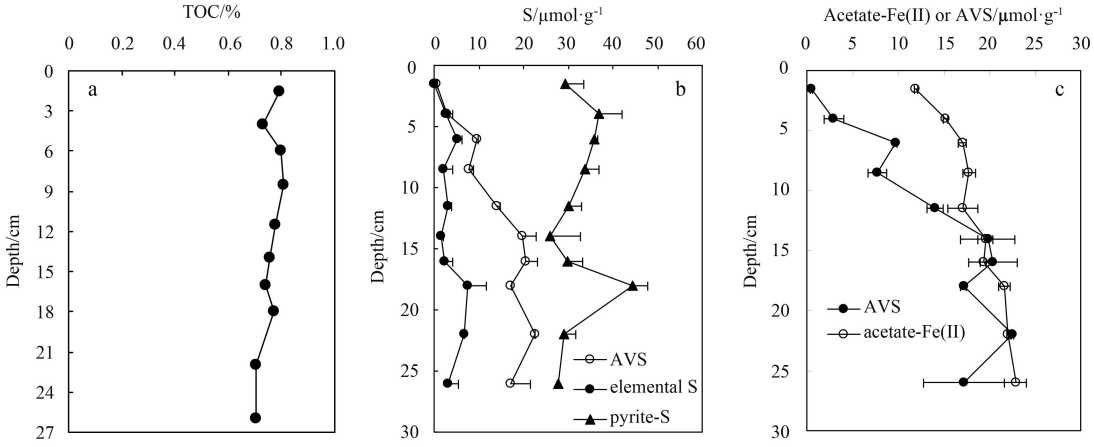

Fig. 3. Content profiles of TOC (a), AVS (b), elemental S (b), pyrite-S (b), and a comparison of AVS and acetate-Fe(II) (c) in Core E6. Error bars represent one standard deviation.

centration in the uppermost 4 cm was low (<3 μmol/g), but increased down-core to 20.4 μmol/g at 16 cm (Fig. 3b), below which the AVS concentrations remained almost invariable. S^0 concentration was relatively low (<7.6 μmol/g) but measurable over the entire core. Pyrite-S concentration was 27–45 μmol/g, much higher than those of AVS and S^0 in the uppermost layer.

Acetate-Fe(II) concentration displayed a gradual down-core increase from 12 to 23 μmol/g (Fig. 3c). $Fe(III)_{am}$ concentration displayed a quick down-core decrease from 9 to 3 μmol/g within the upper 6 cm, and then a gradual decrease to low values at depth (Fig. 4a). Magnetite concentration exhibited a clear down-core decrease over 14 cm depth (Fig. 4b), and then a small de-

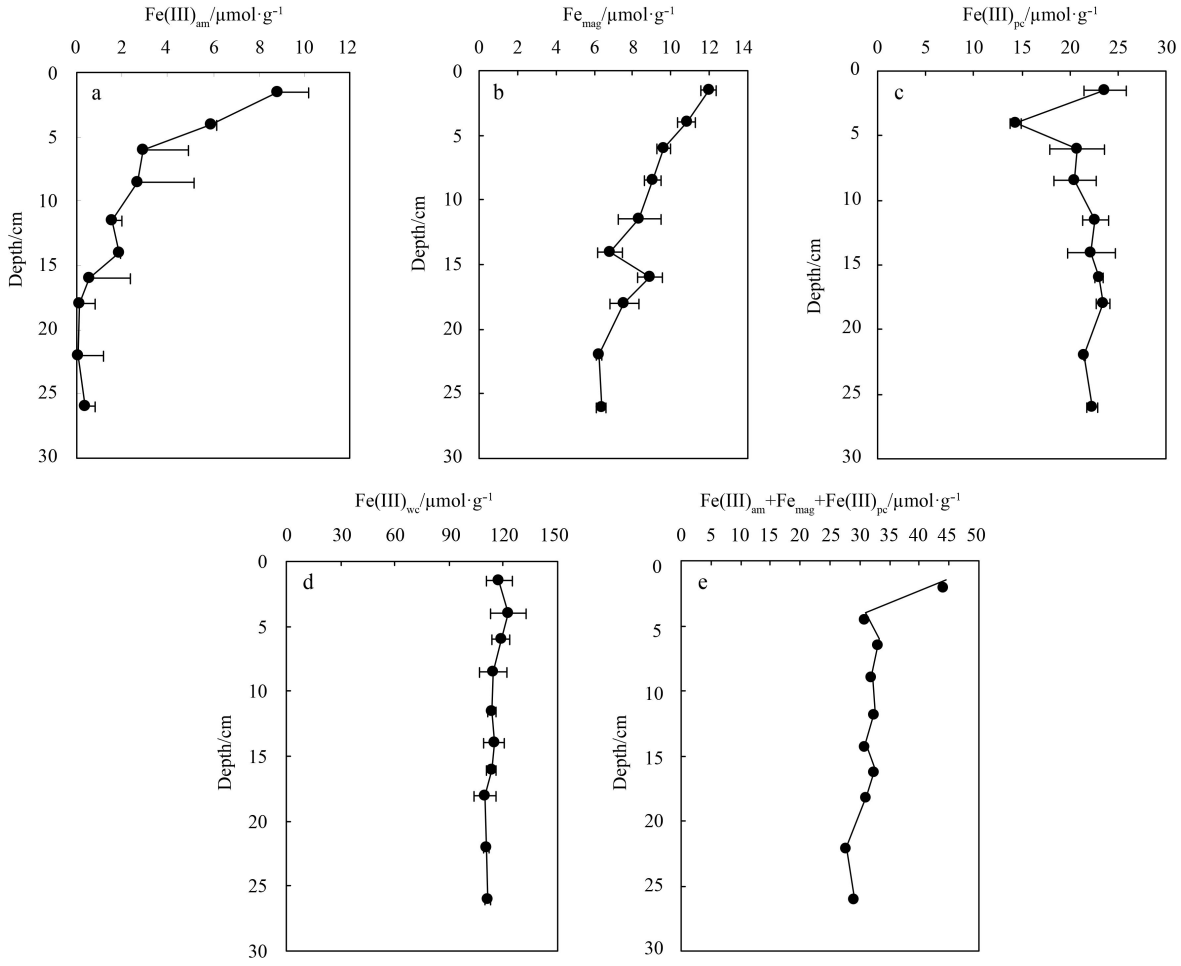

Fig. 4. Concentration profiles of various Fe species. a. amorphous Fe(III) oxides [$Fe(III)_{am}$], b. magnetite-Fe (Fe_{mag}), c. poorly crystalline Fe(III) oxides [$Fe(III)_{pc}$], d. well crystalline Fe(III) oxides [$Fe(III)_{wc}$], and e. the sum of Σ[$Fe(III)_{am}$+Fe_{mag}+$Fe(III)_{pc}$] in Core E6. Error bars represent one standard deviation.

crease below the depth. Except for a minimum of 14.3 μmol/g at 4 cm depth (Fig. 4c), $Fe(III)_{pc}$ concentration was in a narrow range of 20.5–23.7 μmol/g. $Fe(III)_{wc}$ concentration was almost invariable over the entire core depth, with an average of (115±4.0) μmol/g (Fig. 4d).

3.2 *Kinetic characterization of Fe(III)-oxide reactivity*

As an example, Fig. 5a shows a representative curve of time-dependent reductive dissolution of Fe(III) oxides in the core sediments. The optimized values of m_0 and k' were 9.5–14.5 μmol/g and 2×10^{-4}–5.2×10^{-4} s^{-1}, respectively (Figs 5b and c). m_0 does not exhibit a clear depth variability except a quick decrease from the uppermost layer to a depth of 5 cm. k' remains stable over the upper 5 cm, but displays down-core decrease below this depth.

4 Discussion

4.1 *Sulfur diagenesis and the importance of MIR*

Despite enhanced primary production due to eutrophication of the bay, the TOC content in the core was not markedly different from TOC average (0.75 %) for world shelf sediments (Berner, 1982). Almost constant TOC contents over the core (Fig. 3a) may be indicative of low degradability of the OM. AVS and pyrite-S contents in the core were similar to those in the East China Sea (ECS) (Zhu et al., 2013), but were at the lower end for normal marine sediments (Goldhaber, 2003) and much lower than in some marine sediments impacted by eutrophication (Zimmerman and Canuel, 2000; Kraal et al., 2013). Both TOC and reduced S in the core seemingly indicate that eutrophication has not enhanced burial of labile OM and reduced S in the sediment due to excessive consumption of labile OM by large-scale shellfish mariculture (Liu et al., 2010), in consistent with previous observation at other sites of the bay (Zhu et al., 2014a).

Low concentrations of AVS and S^0 over the upper core (Fig. 3b) may be a net result of low sulfate reduction rates, conversion of AVS and S^0 to pyrite, and reoxidation of AVS and S^0 (Rickard and Morse, 2005). The depth profile of pyrite-S generally exhibits no significant variability, though a peak of pyrite-S was observed at 18 cm depth, which could be ascribed to a local heterogeneity of labile OM. This implies that pyrite formation has occurred mainly over the uppermost layer, below which its formation has not proceeded to a great extent. Pyrite formation may go through several possible pathways (Rickard, 2014). The coexistence of AVS and S^0 in the sediments may have favored the polysulfide pathway (Eqs (4) and (5)) (e.g., Luther III, 1991; Rickard, 1975).

$$FeS + S^0 = FeS_2, \tag{4}$$

$$FeS + S_n^{2-} = FeS_2 + S_{n-1}^{2-}. \tag{5}$$

Acetate-Fe(II) concentrations were much higher than those

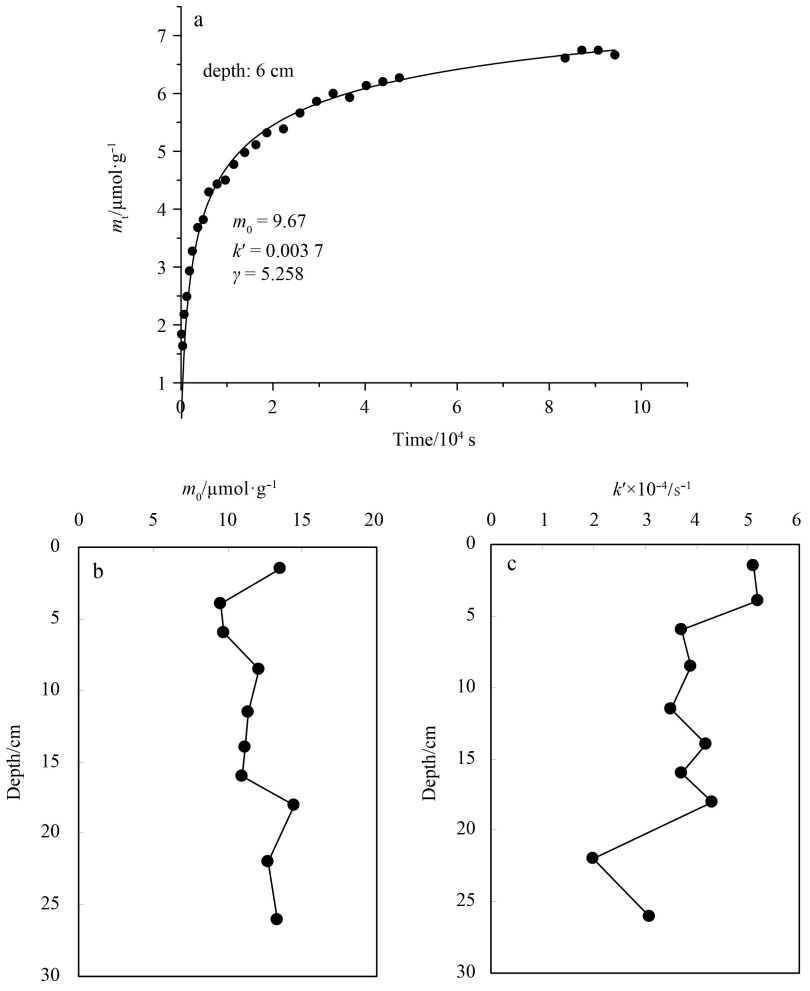

Fig. 5. Representative curve of time-dependent dissolution of sedimentary Fe(III) oxides by buffered ascorbate (pH 7.5) at the depth of 6 cm (a), profiles of m_0 (b) and k' (c) in Core E6.

of AVS over the upper 12 cm (Fig. 3c), whereas they were comparable below 14 cm depth. Given that Fe(II) sulfides (pyrite excluded) occur mainly as FeS (namely, Fe to S molar ratio is 1:1), the AVS and the above acetate-Fe(II) profiles suggest that a portion of acetate-Fe(II) remained non-sulfidized in the upper layer, while acetate-Fe(II) has been almost quantitatively sulfidized in the deeper layer. The dominance of non-sulfidized Fe(II) over the upper layer unequivocally suggests that the porewater was sulfide-starved, otherwise the acetate-Fe(II) would be comparable to, or lower than, the AVS contents as a result of quantitative sulfidization of reduced Fe. The result is in consistent with our previous observation that porewater sulfide at a nearby site (J1) was below the detection limit (<1 μmol/dm^3) (Zhu et al., 2012). In addition, though highly heterogeneous dissolved sulfide distributions are generally expected in marine sediments, circumstance evidence (Pu et al., 2009; Chen et al., 2014, Zhu et al., 2015) consistently suggests that detectable dissolved sulfide is restricted to the mouths of the Licun River and the Haibo River at the eastern Jiaozhou Bay, which have been impacted by inputs of domestic and industrial sewages, while dissolved sulfide is generally undetectable beyond the mouths. The dominance of non-sulfidized Fe(II) also implies that MIR may have prevailed and been mainly responsible for the production of non-sulfidized Fe(II) in the upper sulfide-starved layer. This is quite different from the cases of many other eutrophic coastal settings, where enriched labile OM in the sediments usually renders sulfate reduction solely important in OM oxidation (Álvarez-Iglesias and Rubio, 2012; Kraal et al., 2013; Lehtoranta et al., 2009). The above difference may be due to low degradability of OM and/or high availability of FeO_{HR} (see below). With increasing depth, sulfate reduction was expected to be more active and eventually to outcompete MIR. As a result, Fe(III) oxides were mainly reduced by dissolved sulfide, and the consequential Fe^{2+} was quantitatively precipitated as Fe(II) sulfides (Fig. 3c).

4.2 *Partitioning and diagenetic variations of Fe(III) oxides*

$Fe(III)_{am}$, $Fe(III)_{pc}$, Fe_{mag}, and $Fe(III)_c$ are considered as FeO_{HR} (März et al., 2012; Poulton and Canfield, 2005). Among the four FeO_{HR} phases, $Fe(III)_{am}$ is the most reactive pool and thus is always preferentially reduced in anoxic settings, which is supported by its quick down-core decrease and depletion at 14 cm depth (Fig. 4a). As earlier demonstrated, the dominance of non-sulfidized acetate-Fe(II) over the upper centimeters suggests that MIR may be mainly responsible for $Fe(III)_{am}$ reduction in the interval. Note that low contents of AVS and pyrite in the same depth interval indicate that sulfate reduction has also occurred. That is understandable given the fact that although MIR is thermodynamically more favored, it usually does not completely inhibit sulfate reduction because MIR is limited to microniches around Fe oxide particulates, while sulfate reducers can cluster around any other organic-rich hotspots and reduce sulfate without risking depletion of their electron acceptor due to high diffusivity of sulfate ions (Hoehler et al., 1998; Thamdrup, 2000).

$Fe(III)_{pc}$ is also readily reduced by both CIR and MIR in anoxic settings (März et al., 2012; Poulton and Canfield, 2005), but the minimum of $Fe(III)_{pc}$ (Fig. 4c) may indicate that intensive reductive loss of $Fe(III)_{pc}$ has been restricted to a thin layer beneath the redox interface. Given the high reactivity of $Fe(III)_{pc}$, no depletion of this pool at depth implies that FeO_{HR} availability is not a limiting factor of Fe(III) reduction.

In marine sediments, magnetite is found as a detrital phase from rock weathering and/or as biogenic mineral (Canfield and Berner, 1987; Konhauser, 2006). Regardless of the sources of magnetite in the core, a down-core decrease in Fe_{mag} concentration (Fig. 4b) indicates the occurrence of its diagenetic dissolution. Similar observations have been reported in other marine sediments (Canfield and Berner, 1987; Rowan et al., 2009). As compared with the depth of magnetite dissolution (≈1 m) in the ECS fluidized mud (Ge et al., 2015), the depth in the bay sediments is much shallower due probably to more reducing condition.

$Fe(III)_{wc}$ concentrations are much higher than the other FeO_{HR} pools. Invariable concentrations of this phase over the entire core indicate that it is barely involved in Fe reduction. This is understandable because, as earlier demonstrated, much more reactive $Fe(III)_{pc}$ has not yet become depleted over the whole depths studied, it is highly impossible for $Fe(III)_{wc}$ to be reduced to a great extent.

As demonstrated above, only three Fe(III)-bearing pools, that is, $Fe(III)_{am}$, $Fe(III)_{pc}$, and Fe_{mag}, have been involved in diagenetic reduction. A marked down-core decrease of the sum of three pools appeared only within the upper 4 cm (Fig. 4e), suggesting that the significant diagenetic reduction has been restricted to the uppermost layer.

Combination of the evidence of above AVS, Fe(II), and $Fe(III)_{am}$ highlights the importance of MIR in the upper sediment layer. It has been established that low to intermediate availability of labile OM but high availability of FeO_{HR} are required for the prevalence of MIR in marine settings (Jensen et al., 2003; Nickel et al., 2008; Thamdrup, 2000). In the case of this study, the importance of MIR over the upper layer may be a combined result of high availability of FeO_{HR} and low availability of labile OM. First, previous results have shown that FeO_{HR} is enriched to some extent in the semienclosed bay relative to average marine sediment (Zhu et al., 2015), which may have favored MIR in the site. Second, large-scale shellfish mariculture near the site may have prevented enrichment of labile OM in the sediments despite eutrophication of the water. As a result, low to intermediate availability of labile OM may also have encouraged the MIR. Thus the low to intermediate availability of labile OM is the ultimate factor limiting the rate of sulfate reduction and low accumulation of reduced sulfur (AVS, S^0, and pyrite).

4.3 *Pool size and reactivity of MR-Fe(III)*

As indicated earlier, the size of MR-Fe(III) is a maximum estimate of MR-Fe(III) present in the sediments. The sizes were larger than $Fe(III)_{am}$ but smaller than $Fe(III)_{pc}$ contents. A marked depletion of $Fe(III)_{am}$ below 10 cm depth has not resulted in a decrease in the MR-Fe(III) over the depth, implying that besides the most bioavailable $Fe(III)_{am}$, a portion of less reactive Fe(III) phases such as $Fe(III)_{pc}$ is also an important contributor to the MR-Fe(III). Note that abundant availability of MR-Fe(III) has not supported continuous MIR below a depth larger than 15 cm, as indicated by almost quantitative sulfidization of Fe(II) (Fig. 3c). This supports the earlier speculation that MIR has been outcompleted by CIR due to enhanced sulfate reduction in the deeper layer.

The k' profile revealed an overall decrease in reactivity, particularly from the subsurface to the bottom of the core (Fig. 5c). In anoxic settings, FeO_{HR}, particularly $Fe(III)_{am}$, is always preferentially reduced, leaving less reactive Fe(III)-oxide phases largely intact. As a result, k' shows a down-core decrease as expected. A comparison of the k' with those for some synthetic minerals may provide mineralogical information on MR-Fe(III) of the core. Up to date, ferrihydrite and amorphous $Fe(PO_4)_{0.7}$ are the only syn-

thetic Fe(III)-bearing phases whose k' at pH 7.5 has been determined (Hyacinthe and van Cappellen, 2004; Raiswell et al., 2010). The k' values for the core were much lower than those (10.3×10^{-4} s^{-1}) for fresh ferrihydrite (Raiswell et al., 2010) and amorphous $Fe(PO_4)_{0.7}$ (10×10^{-4} s^{-1}) (Hyacinthe and van Cappellen, 2004), but comparable to that for ferrihydrite after aging for 11 d (4.1×10^{-4} s^{-1}) (Raiswell et al., 2010). It may implies that the overall reactivity of the MR-Fe(III) is mineralogically equivalent to aged ferrihydrite. Note that the MR-Fe(III) is still a heterogeneous assemblage, covering a wide range of reactivity as indicated by down-core decrease in k'.

A case study in Core E6 demonstrates that a combination of refined Fe speciation and quantitative kinetic characterization of reactivity can offer nuanced information on Fe(III) diagenesis from multiple perspectives.

5 Summary and conclusions

The case study indicates that refined Fe speciation together with S speciation in the sediment profile can help to enhance our understanding of Fe and S diagenesis. A combination of refined Fe speciation and quantitative kinetic characterization of reactivity can offer nuanced information on Fe(III) diagenesis from multiple perspectives.

Among the four operational FeO_{HR} phases ($Fe(III)_{am}$, $Fe(III)_{pc}$, Fe_{mag}, and $Fe(III)_{wc}$) in the core studied, $Fe(III)_{wc}$ had the highest contents, followed by $Fe(III)_{pc}$, Fe_{mag}, and $Fe(III)_{am}$. The dominance of nonsulfidized Fe(II) over the upper 12 cm of the core indicates the importance of MIR in the sulfide-starving setting. In the deeper layers, however, almost all reduced Fe has been sulfidized, indicative of the importance of CIR. Both $Fe(III)_{am}$ and $Fe(III)_{pc}$ have been the sources of MIR over the upper layer. $Fe(III)_{wc}$ has almost not been involved in Fe reduction. The profiles of MR-Fe(III), $Fe(III)_{am}$, and $Fe(III)_{pc}$ indicate that both the most reactive $Fe(III)_{am}$ and less reactive $Fe(III)_{pc}$ are an important contributors to MR-Fe(III). The MR-Fe(III) in the site is mineralogically analogous to aged ferrihydrite, but is still a heterogeneous assemblage with decreasing reactivity with depth.

Evidence from TOC, reduced S, FeO_{HR}, and MR-Fe(III) together indicates that the importance of MIR over the upper layer may be a combined result of high availability of FeO_{HR} and low availability of labile OM.

References

Álvarez-Iglesias P, Rubio B. 2012. Early diagenesis of organic-matter-rich sediments in a ría environment: organic matter sources, pyrites morphology and limitation of pyritization at depth. Estuarine, Coastal and Shelf Science, 100: 113–123

Amann R, Glöckner F O, Neef A. 1997. Modern methods in subsurface microbiology: in situ identification of microorganisms with nucleic acid probes. FEMS Microbiology Reviews, 20(3-4): 191–200

Beckler J S, Kiriazi N, Rabouille C, et al. 2016. Importance of microbial iron reduction in deep sediments of river-dominated continental-margins. Marine Chemistry, 178: 22–34

Berner R A. 1982. Burial of organic carbon and pyrite sulfur in the modern ocean: its geochemical and environmental significance. American Journal of Science, 282(4): 451–473

Burton E D, Sullivan L A, Bush R T, et al. 2008. A simple and inexpensive chromium-reducible sulfur method for acid-sulfate soils. Applied Geochemistry, 23(9): 2759–2766

Canfield D E, Berner R A. 1987. Dissolution and pyritization of magnetite in anoxie marine sediments. Geochimica et Cosmochimica Acta, 51(3): 645–659

Canfield D E, Kristensen E, Thamdrup B. 2005. Aquatic Geomicrobiology. Amsterdam: Elsevier

Chen Liangjin, Zhu Maoxu, Yang Guipeng, et al. 2013. Reductive reactivity of iron(III) oxides in the East China Sea sediments: characterization by selective extraction and kinetic dissolution. PLoS One, 8(11): e80367

Chen Keke, Zhu Maoxu, Yang Guipeng, et al. 2014. Spatial distribution of organic and pyritic sulfur in surface sediments of eutrophic Jiaozhou Bay, China: clues to anthropogenic impacts. Marine Pollution Bulletin, 88(1-2): 284–291

Cline J D. 1969. Spectrophotometric determination of hydrogen sulfide in natural waters. Limnology and Oceanography, 14(3): 454–458

Devereux R, Lehrter J C. 2015. Manganese, iron, and sulfur cycling in Louisiana continental shelf sediments. Continental Shelf Research, 99: 46–56

Ge Can, Zhang Weiguo, Dong Chenyin, et al. 2015. Magnetic mineral diagenesis in the river-dominated inner shelf of the East China Sea, China. Journal of Geophysical Research: Solid Earth, 120(7): 4720–4733

Goldhaber M B. 2003. Sulfur-rich sediment. In: Mackenzie F T, ed. Sediments, Diagenesis, and Sedimentary Rocks, Treatise on Geochemistry. Amsterdam: Elsevier, 257–288

Hoehler T M, Alperin M J, Albert D B, et al. 1998. Thermodynamic control on hydrogen concentrations in anoxic sediments. Geochimica et Cosmochimica Acta, 62(10): 1745–1756

Hyacinthe C, Bonneville S, van Cappellen P. 2006. Reactive iron(III) in sediments: chemical versus microbial extractions. Geochimica et Cosmochimica Acta, 70(16): 4166–4180

Hyacinthe C, van Cappellen P. 2004. An authigenic iron phosphate phase in estuarine sediments: composition, formation and chemical reactivity. Marine Chemistry, 91(1-4): 227–251

Hyun J H, Kim S H, Mok J S, et al. 2013. Impacts of long-line aquaculture of Pacific oysters (*Crassostrea gigas*) on sulfate reduction and diffusive nutrient flux in the coastal sediments of Jinhae-Tongyeong, Korea. Marine Pollution Bulletin, 74(1): 187–198

Jacobson M E. 1994. Chemical and biological mobilization of Fe(III) in marsh sediments. Biogeochemistry, 25(1): 40–60

Jensen M M, Thamdrup B, Rysgaard S, et al. 2003. Rates and regulation of microbial iron reduction in sediments of the Baltic-North Sea transition. Biogeochemistry, 65(3): 295–317

Kallmeyer J, Ferdelman T G, Weber A, et al. 2004. A cold chromium distillation procedure for radiolabeled sulfide applied to sulfate reduction measurements. Limnology and Oceanography: Methods, 2(6): 171–180

Konhauser K. 2006. Introduction to Geomicrobiology. Malden: Blackwell Publishing

Koretsky C M, Moore C M, Lowe K L, et al. 2003. Seasonal oscillation of microbial iron and sulfate reduction in saltmarsh sediments (Sapelo Island, GA, USA). Biogeochemistry, 64(2): 179–203

Koretsky C M, van Cappellen P, DiChristina T J, et al. 2005. Salt marsh pore water geochemistry does not correlate with microbial community structure. Estuarine, Coastal and Shelf Science, 62(1-2): 233–251

Kostka J E, Luther III G W. 1994. Partitioning and speciation of solid phase iron in saltmarsh sediments. Geochimica et Cosmochimica Acta, 58(7): 1701–1710

Kraal P, Burton E D, Bush R T. 2013. Iron monosulfide accumulation and pyrite formation in eutrophic estuarine sediments. Geochimica et Cosmochimica Acta, 122: 75–88

Kristensen E, Mangion P, Tang M, et al. 2011. Microbial carbon oxidation rates and pathways in sediments of two Tanzanian mangrove forests. Biogeochemistry, 103(1): 143–158

Larsen O, Postma D. 2001. Kinetics of reductive bulk dissolution of lepidocrocite, ferrihydrite, and goethite. Geochimica et Cosmochimica Acta, 65(9): 1367–1379

Lehtoranta J, Ekholm P, Pitkänen H. 2009. Coastal eutrophication thresholds: a matter of sediment microbial processes. Ambio, 38(6): 303–308

Liu Sumei, Zhang Jing, Chen Hongtao, et al. 2005. Factors influencing nutrient dynamics in the eutrophic Jiaozhou Bay, North China. Progress in Oceanography, 66(1): 66–85

Liu Sumei, Zhu Bingde, Zhang Jing, et al. 2010. Environmental

change in Jiaozhou Bay recorded by nutrient components in sediments. Marine Pollution Bulletin, 60(9): 1591–1599

Lovley D R. 1991. Dissimilatory Fe(III) and Mn(IV) reduction. Microbiological Review, 55(2): 259–287

Lovley D R, Phillips E J P. 1987. Rapid assay for microbially reducible ferric iron in aquatic sediments. Applied and Environmental Microbiology, 53(7): 1536–1540

Luna G M, Manini E, Danovaro R. 2002. Large fraction of dead and inactive bacteria in coastal marine sediments: comparison of protocols for determination and ecological significance. Applied and Environmental Microbiology, 68(7): 3509–3513

Luther III G W. 1991. Pyrite synthesis via polysulfide compounds. Geochimica et Cosmochimica Acta, 55(10): 2839–2849

März C, Poulton S W, Brumsack H J, et al. 2012. Climate-controlled variability of iron deposition in the central arctic ocean (southern Mendeleev Ridge) over the last 130 000 years. Chemical Geology, 330-331: 116–126

Nickel M, Vandieken V, Brüchert V, et al. 2008. Microbial Mn(IV) and Fe(III) reduction in northern Barents Sea sediments under different conditions of ice cover and organic carbon deposition. Deep-Sea Research: Part II Topical Studies in Oceanography, 55(20-21): 2390–2398

Postma D. 1993. The reactivity of iron oxides in sediments: a kinetic approach. Geochimica et Cosmochimica Acta, 57(21-22): 5027–5034

Poulton S W, Canfield D E. 2005. Development of a sequential extraction procedure for iron: implications for iron partitioning in continentally derived particulates. Chemical Geology, 214(3-4): 209–221

Pu Xiaoqiang, Zhong Shaojun, Liu Fei, et al. 2009. Restriction factors to sulfide formation in estuarine sediments of Licun River of Jiaozhou Bay. Geochimica (in Chinese), 38(4): 323–333

Raiswell R, Canfield D E. 2012. The iron biogeochemical cycle past and present. Geochemical Prospectives, 1(1): 1–220

Raiswell R, Canfield D E, Berner R A. 1994. A comparison of iron extraction methods for the determination of degree of pyritisation and the recognition of iron-limited pyrite formation. Chemical Geology, 111(1–4): 101–110

Raiswell R, Vu H P, Brinza L, et al. 2010. The determination of labile Fe in ferrihydrite by ascorbic acid extraction: methodology, dissolution kinetics and loss of solubility with age and de-watering. Chemical Geology, 278(1-2): 70–79

Rickard D T. 1975. Kinetics and mechanism of pyrite formation at low temperatures. American Journal of Science, 275(6): 636–652

Rickard D. 2014. The sedimentary sulfur system: biogeochemistry and evolution through geologic time. In: Mackenzie F T, ed. Sediments, Diagenesis, and Sedimentary Rocks, Treatise on Geochemistry. 2nd ed. Amsterdam: Elsevier, 267–326

Rickard D, Morse J W. 2005. Acid volatile sulfide (AVS). Marine Chemistry, 97(3-4): 141–197

Rowan C J, Roberts A P, Broadbent T. 2009. Reductive diagenesis, magnetite dissolution, greigite growth and paleomagnetic smoothing in marine sediments: a new view. Earth and Planetary Science Letters, 277(1-2): 223–235

Rysgaard S, Fossing H, Jensen M M. 2001. Organic matter degradation through oxygen respiration, denitrification, and manganese, iron, and sulfate reduction in marine sediments (the Kattegat and the Skagerrak). Ophelia, 55(2): 77

Stookey L L. 1970. Ferrozine -A new spectrophotometric reagent for iron. Analytical Chemistry, 42(7): 779–781

Thamdrup B. 2000. Bacterial manganese and iron reduction in aquatic sediments. In: Schink B, eds. Advances in Microbial Ecology. New York: Springer, 41–84

Wang Yifeng, van Cappellen P. 1996. A multicomponent reactive transport model of early diagenesis: application to redox cycling in coastal marine sediments. Geochimica et Cosmochimica Acta, 60(16): 2993–3014

Wijsman J W M, Herman P M J, Middelburg J J, et al. 2002. A model for early diagenetic processes in sediments of the continental shelf of the Black Sea. Estuarine, Coastal and Shelf Science, 54(3): 403–421

Wu Yulin, Sun Song, Zhang Yongshan. 2005. Long-term change of environment and it's influence on phytoplankton community structure in Jiaozhou Bay. Oceanologia et Limnologia Sinica (in Chinese), 36(6): 487–498

Zhu Maoxu, Chen Liangjin, Yang Guipeng, et al. 2014a. Humic sulfur in eutrophic bay sediments: characterization by sulfur stable isotopes and K-edge XANES spectroscopy. Estuarine, Coastal and Shelf Science, 138: 121–129

Zhu Maoxu, Chen Liangjin, Yang Guipeng, et al. 2014b. Kinetic characterization on reductive reactivity of iron(III) oxides in surface sediments of the East China Sea and the influence of repeated redox cycles: implications for microbial iron reduction. Applied Geochemistry, 42: 16–26

Zhu Maoxu, Huang Xiangli, Yang Guipeng, et al. 2015. Iron geochemistry in surface sediments of a temperate semi-enclosed bay, North China. Estuarine, Coastal and Shelf Science, 165: 25–35

Zhu Maoxu, Liu Juan, Yang Guipeng, et al. 2012. Reactive iron and its buffering capacity towards dissolved sulfide in sediments of Jiaozhou Bay, China. Marine Environmental Research, 80: 46–55

Zhu Maoxu, Shi Xiaoning, Yang Guipeng, et al. 2013. Formation and burial of pyrite and organic sulfur in mud sediments of the East China Sea inner shelf: constraints from solid-phase sulfur speciation and stable sulfur isotope. Continental Shelf Research, 54: 24–36

Zimmerman A R, Canuel E A. 2000. A geochemical record of eutrophication and anoxia in Chesapeake Bay sediments: anthropogenic influence on organic matter composition. Marine Chemistry, 69(1-2): 117–137